DOI: 10.1002/chem.200801113

Synthesis of Nanocrystalline MFI-Zeolites with Intracrystal Mesopores and Their Application in Fine Chemical Synthesis Involving Large Molecules

Rajendra Srivastava, Nobuhiro Iwasa, Shin-ichiro Fujita, and Masahiko Arai *[a]

Heterogeneous catalysts are widely used in petroleum refinery industries and for the production of fine chemicals. However, challenges remain to maximize their efficiency. Microporous crystalline aluminosilicate, zeolites, are widely used as shape-selective catalysts, ion-exchange materials and adsorbents for organic compounds.[1] Their superior performance can often be attributed to the existence of a well-defined system of micropores (size below 2 nm in diameter) with uniform shape and size, typically of molecular dimensions. However, for some applications, the presence of such micropores alone can also result in an unacceptably slow diffusion of reactants and products to and from the active sites located inside the zeolite crystals.[2] To overcome this diffusion limitation, researchers have pursued several different preparative strategies. One approach is to increase the pore size of the zeolite. The mesoporous structure is very promising for reactions involving large molecular species, owing to the possibility of overcoming the diffusion limitation in crystalline microporous zeolites (0.4–1.5 nm in pore diameter). The most common and successful approach so far is to introduce an additional system of mesopores (sizes between 2 and 50 nm) into each individual zeolite crystal.[3–7] This is typically done by suitable post-treatments such as steaming[3] and chemical etching routes.[4] Mesopores can be introduced directly into the zeolite crystals, without a partially destructive post-treatment, simply by conducting the crystallization in the presence of mesoporous carbon and using carbon nanotubes as a hard template.[5] The carbon particles are encapsulated by the zeolite crystals during growth. After complete crystallization, the carbon template is easily removed by combustion to produce highly mesoporous zeolite single crystals that combine most of the desirable catalytic properties of zeolites and mesoporous molecular sieves. The direct synthesis of a zeolite with tunable mesoporosity by using organosilane surfactants as a mesopore director has very recently been reported.[6] The resultant zeolites are highly mesoporous, and the mesopore walls show the characteristics of a fully crystalline zeolite framework. The mesopore diameters are tunable by the chain length of the surfactants used. This MFI-zeolite with a mesoporous/microporous hierarchical structure shows a remarkably improved resistance to the deactivation of catalytic activities in various reactions.[7] In addition, the hierarchical MFI-zeolite exhibits very high catalytic activity in the synthesis of large molecules for which conventional zeolite materials are inactive and conventional mesoporous materials are less active. Another approach to improve the catalytic activity is to minimize the size of the zeolite crystals and thereby shorten the diffusion path.[8]

The present study is based on the second approach in which the size of zeolite nanocrystals is reduced to 20 nm by adding alkyltriethoxysilane into the conventional zeolite synthesis gel. Crystal size of MFI-zeolite was effectively controlled by the addition of alkyltriethoxysilanes (alkyl = methyl, propyl and octyl) into a hydrothermal synthesis mixture of conventional MFI-zeolite. The materials obtained exhibit remarkably enhanced catalytic activities in several organic reactions involving large molecules. Here, we have shown that the alkyltriethoxysilanes mediated synthesis method can be effectively used to control the size of the zeolite crystals, particle morphology, and mesoporosity.

First, a conventional MFI was hydrothermally prepared at 443 K by using tetraethylorthosilicate (TEOS) and tetrapropylammonium hydroxide (TPAOH) (gel composition $TEOS/Al_2O_3/Na_2O/TPAOH/H_2O$: 100:2.5:3.3:25:2500). Later, different zeolite samples were prepared with alkyltriethoxysilane (ATES) using different gel compositions ($TEOS/ATES/Al_2O_3/Na_2O/TPAOH/H_2O$: $100-x:x:2.5:3.3:25:2500$, $x = 0-15$). The product was designated by MFI-xATES according to the number of moles (x) of the alkyltriethoxysilane used. All the synthesized zeolites

[a] Dr. R. Srivastava, Dr. N. Iwasa, Dr. S.-i. Fujita, Prof. M. Arai
Division of Chemical Process Engineering
Graduate School of Engineering
Hokkaido University
Sapporo, 060-8628 (Japan)
Fax: (+81) (0)11-706-6595
E-mail: marai@eng.hokudai.ac.jp

Supporting information for this article is available on the WWW under http://dx.doi.org/10.1002/chem.200801113.

had the MFI structure with high phase purity, as confirmed by XRD patterns of Figure 1 (and Figure S1 in the Supporting Information). Zeolite particles with capsule-like crystal

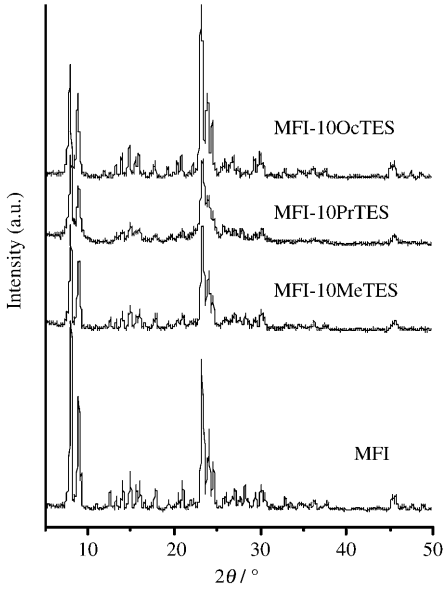

Figure 1. XRD patterns of conventional MFI and MFI samples synthesized using alkyltriethoxysilanes.

morphology were obtained when synthesis was performed without any additive under the present conditions (Figures 2a and 3a,b). The sample prepared with ATES has spherical/egg-shaped nanocrytalline morphology (Figure 2 and 3). The amount of ATES was found to have a high impact on the quality of the samples, as shown by scanning electron microscopy (SEM) analysis (Figure 2). No improvement in crystal morphology was observed when the sample (MFI-2.5PrTES) was prepared using 2.5 mol% propyltriethoxysilane (PrTES) with respect to TEOS (Figure 2 b). When the amount of PrTES was increased to 5.0 mol%, then spherical macroporous zeolite particles (MFI-5PrTES) of about 300 nm diameter were observed (Figure 2c). At 10 mol% loading of PrTES, the zeolite particles (MFI-10PrTES) exhibit a round/egg shape with a nanoscale jagged surface. The SEM and transmission electron microscopy (TEM) images show that the round/egg shape particles were built with an assembly of tiny crystallites about 20 nm in diameter or less (Figure 2d, e and 3c,d). However, on further increase in PrTES concentration to 15 mol%, we did not obtain any MFI-zeolite (MFI-15PrTES) (Figure 2 f), as confirmed by XRD (Figure S1 in the Supporting Information). We have also studied the influence of hydrophobicity of ATES by varying the alkyl chain length in ATES used in the synthesis. If the synthesis was performed with 10 mol% methyltriethoxysilane (MeTES), the product (MFI-10MeTES) showed quite uniform, spherical particles that also looked like assembled by nanosize crystallites similar to the sample MFI-10PrTES. As seen in Figure 2(g), the primary building blocks (crystallites) were somewhat bigger in MFI-

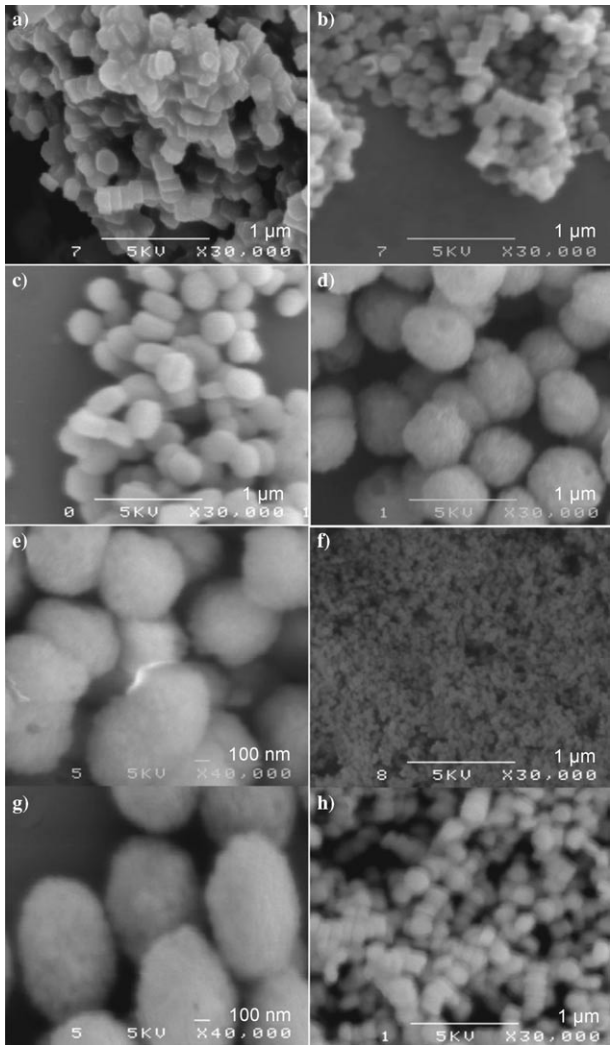

Figure 2. SEM images of conventional MFI and MFI prepared with alkyltriethoxysilanes: a) conventional MFI, b) MFI-2.5PrTES, c) MFI-5PrTES, d,e) MFI-10PrTES, f) MFI-15PrTES, g) MFI-10MeTES, and h) MFI-10OcTES.

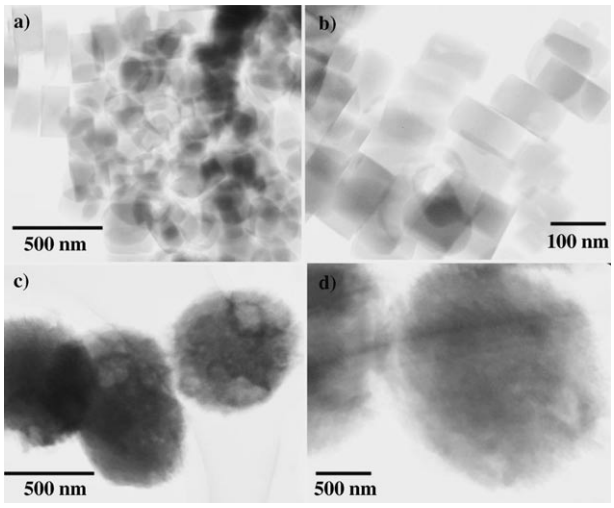

Figure 3. TEM images of a,b) conventional MFI and c,d) MFI-10PrTES.

10MeTES than in MFI-10PrTES. The TEM image of MFI-10PrTES clearly showed a nanocrystal-mesopore alternating framework structure (Figure 3c,d). If the sample (MFI-10OcTES) was prepared with 10 mol% octyltriethoxysilane, the size of the crystal decreased, but no morphological changes were observed (Figure 2 h).

The N_2-adsoption results reveal that external surface area and pore volume increase proportionally with the concentration of ATES (Table 1). The N_2-adsoption isotherm for MFI-10PrTES showed a typical type-IV isotherm similar to the mesoporous silica materials (Figure 4). The major difference of this isotherm from that of conventional MFI is a distinct increase of N_2 adsorption in the region $0.4 < P/P_o < 0.9$, which is interpreted as capillary condensation in mesopore void spaces. The mesopores show a pore size distribution in the range of 3–8 nm. As evidenced from the SEM and TEM images, the mesopores correspond to the void space between nanosized crystal domains inside a zeolite particle.

Table 1. Textural characteristics of MFI and MFI prepared with alkyltriethoxysilane.

Sample	Si/Al[a]	Total surface area [$m^2 g^{-1}$]	External surface area [$m^2 g^{-1}$][b]	Micropore volume [$cc g^{-1}$][b]	Total pore volume [$cc g^{-1}$]
MFI	24.0	304	53	0.124	0.211
MFI-2.5PrTES	–	318	62	0.130	0.219
MFI-5PrTES	–	387	127	0.132	0.295
MFI-10PrTES	26.3	526	262	0.120	0.427
MFI-10MeTES	29.2	486	171	0.125	0.343
MFI-10OcTES	33.4	388	125	0.134	0.254

[a] Si/Al ratio was obtained by ICP analysis; [b] calculated by t-plot method.

^{27}Al and ^{29}Si MAS NMR results show that all the samples contain only tetrahedral aluminium sites and most of the Si is in Si(0Al) environment. Si(1Al) species were also detected in some quantity in each sample (Figure S2 and S3 in the Supporting Information). The temperature-programmed desorption (TPD) of NH_3 was measured to characterize the acidity of the MFI samples. The results obtained are given in Figure S4 and Table S1 of the Supporting Information.

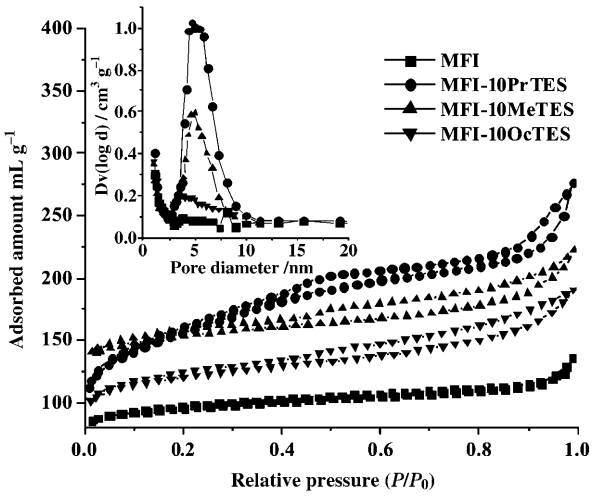

Figure 4. N_2 isotherms of conventional MFI and MFI prepared with alkyltriethoxysilanes (inset: pore size distribution of the corresponding samples).

A previous study based on biominerallization processes[9] and some successful synthesis works[10] suggest that organic molecules that have a strong interaction with the growing crystal surface can effectively modulate the crystallization process of inorganic materials. Therefore, we have chosen some commercially available alkyltriethoxysilane molecules to enhance the interaction with growing zeolite crystals. The idea behind choosing such alkyltriethoxysilane molecules is that it contains a hydrolysable alkoxysilyl moiety. It is expected that it could strongly interact with growing crystal domains through the formation of covalent bonds with other SiO_2 and Al_2O_3 sources using the alkoxysilyl moiety. The present SEM, TEM and N_2-adsorption studies show that the zeolite samples prepared with PrTES and MeTES have a spherical/egg-shape morphology, which is built with nanosized zeolite crystals and that mesopores are present in the void space between nanocrystals inside the zeolite particle. Such a nanocrystal-mesopore alternating-framework structure is not likely to be formed if the distribution of the organic groups is homogeneous throughout the entire zeolite particle. Therefore, it may be proposed that the mesoporous-zeolite crystallization was mediated by the nanoscale segregation of organic-rich and organic-lean domains on the growing zeolite particles. The alkylalkoxysilanes contain only three hydrolyzable moieties (with one hydrophobic alkyl group), which is disadvantageous for the formation of extended tetrahedral SiO_2 linkages. Consequently, the zeolite growth might be significantly retarded at the organic and inorganic interfaces, resulting in the formation of nanocrystal-mesopore alternating frameworks. The surface area of the obtained samples follows the order MFI-10PrTES > MFI-10MeTES > MFI-10OcTES. This clearly indicates that moderate length alkyl-chain-containing organosilanes have a strong interaction with the growing crystals and, hence, effectively modulate the zeolite crystallization to form high surface area nanosized zeolite nanocrystals. The long-alkyl-chain hydrophobic ATES (octyltriethoxysilane) was found to be less effective, as it may be segregated from the aluminosilicate domain and unable to modulate the crystallization process by participating in crystal growth.

The catalytic activities of the zeolite samples prepared with ATES were compared with the conventional MFI-zeolite. Test reactions used included alkylation, condensation and protection reactions (Scheme 1). Using these reactions several synthetic intermediates such as flavanone/chalcone,[11] 7-hydroxy-4-methylcoumarin[12] and diphenyl meth-

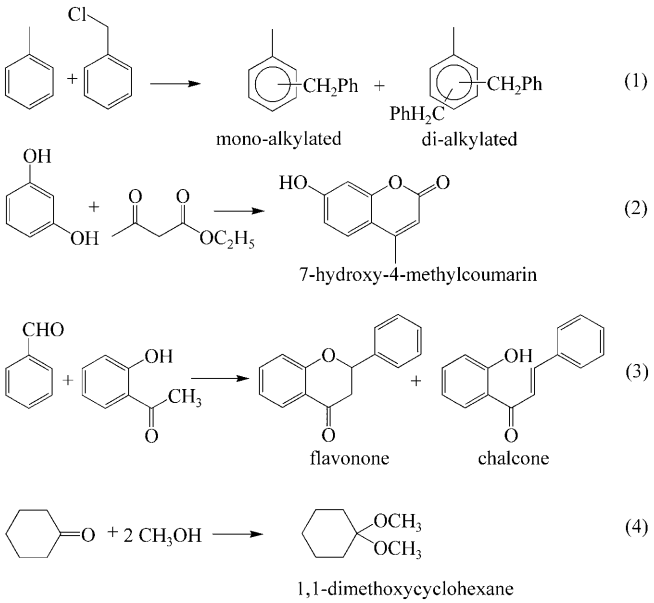

Scheme 1. Catalytic reactions investigated in this study.

ane[13] can be synthesized, which have important relevance in chemical industries. The synthesis of 7-hydroxy-4-methylcoumarin takes place by means of the Pechmann reaction. The reaction proceeds through trans-esterification and intramolecular hydroxyalkylation, followed by dehydration. The synthesis of flavanone occurs through the reaction between 2′-hydroxyacetophenone and benzaldehyde. The first step yields 2′-hydroxychalcone through Claisen–Schmidt condensation. Flavanone is obtained by intramolecular cyclisation of the 2′-hydroxychalcone. The reaction results obtained are summarized in Table 2. For the reactions (1)–(3) (Scheme 1) involving large molecules, the zeolite samples synthesized with ATES were found to be highly active compared to conventional MFI-zeolite. In these reactions, the MFI-10PrTES sample was significantly more active than the other catalysts (Table 2). The total amount of acid sites characterized by the TPD of NH_3 did not correlate with the catalytic activity and so some particular acid sites should be labeled working active sites, and would depend on the reactions examined. At present we do not know the details of the acidity of those active sites and the distribution of them in the mesopores and micropores. However, it may be reasonable to assume that one of important factors responsible for the differences in the catalytic activity (Table 2) is improved mass transport, owing to the presence of intracrystal mesopores. To confirm this aspect, the catalytic activity was examined for protection reaction (Entry 4, Table 2) involving reactants with small molecular dimensions (i.e., methanol and cyclohexanone). In this case, the catalytic activity was found to be very similar for all the catalysts investigated in this study (Table 2). The high catalytic activity of MFI-10PrTES in all the cases may be a result of the formation of smaller zeolite crystallites and the presence of intracrystal mesopores between them, which will shorten the diffusion path and exhibit facile diffusion of product molecules.

In summary, the present study proposes a new method of controlling the nano-crystal size and mesoporosity, by the simple addition of alkyl-alkoxysilanes into conventional zeolite-synthesis composition. The resultant zeolite products have intracrystal mesoporosity and can exhibit significantly enhanced catalytic activities for the synthesis of large molecules that cannot enter zeolite micropores. Propyltriethoxysilane is more effective for the generation of mesoporosity than methyltriethoxysilane and octyltriethoxysilane. It is proposed that the mesoporosity could be generated according to the nanoscale alternation of optimum hydrophobic, organic-rich domains and less hydrophobic inorganic domains, during the crystal growth. Further studies are in progress in our laboratory.

Experimental Section

In a typical synthesis of MFI-zeolite, alkylalkoxysilane (ATES, A = propyl, methyl or octyl, purchased from Aldrich) was mixed with tetrapropylammonium hydroxide (20% TPAOH aq. solution, TCI, Japan) and sodium aluminate solution. The initial mixture was stirred for 15 min at 298 K, until it became a clear solution. Tetraethylorthosilicate (TEOS, Aldrich) was added into the solution and stirring was continued for 6 h. The molar composition of the gel mixture was TEOS/ATES/Al_2O_3/Na_2O/TPAOH/H_2O, $100-x:x$:2.5:3.3:25:2500 (x = 2.5–15). This mixture was transferred to a Teflon-lined autoclave and hydrothermally heated at 443 K for 3 d under static conditions. The final product was filtered, washed with deionised water, and dried at 373 K. The organic template and additives were removed by calcinations at 823 K for 4 h under flowing air. The product was designated by MFI-xPrTES according to the number of moles (x) of the alkyltriethoxysilane. For catalytic applications, the calcined materials were exchanged with NH_4^+ three times using 1 molar NH_4NO_3 solution. Then, the NH_4^+ exchanged-zeolite was calcined again at 823 K to obtain the protonic form of the zeolite.

X-ray diffraction (XRD) patterns of the solid samples prepared were recorded in the 2θ range of 5–70° with a scan speed of 2° min^{-1} by using a Rigaku X-ray diffractometer using $Cu_{K\alpha}$ radiation (λ = 0.1542 nm, 40 kV,

Table 2. Catalytic applications of conventional MFI and MFI samples synthesized using different alkyltriethoxysilanes.

Reactions		MFI	MFI-10MeTES	MFI-10PrTES	MFI-10OcTES
(1)	benzyl chloride conversion [%]	1.6	12.7	33.9	5.2
	mono-alkylated/di-alkylated product	99:1	92:8	89:11	(94:6
(2)	7-hydroxy-4-methylcoumarin [%]	8.5	27.8	50.7	18.6
(3)	2′-hydroxyacetophenone conversion [%]	7.5	16.5	23.8	12.7
	flavanone/chalcone selectivity	65:35	65:35	63:37	63:37
(4)	1,1-dimethoxycyclohexane yield [%]	50.2	57.8	53.7	53.2

Reaction conditions: Methyl substituted diphenylmethane synthesis: toluene (50 mmol); benzyl chloride (5 mmol); catalysts (100 mg); temperature (413 K), runtime (2 h). 7-Hydroxy-4-methylcoumarin synthesis: resorcinol (5 mmol); ethylacetoactetate (7.5 mmol); catalyst (100 mg); temperature (423 K); runtime (4 h). Flavonone/chalcone synthesis: 2′-hydroxyacetophenone (7 mmol); benzaldehyde (7 mmol); catalyst (100 mg); temperature (423 K); runtime (8 h); Protection reaction: cyclohexanone (5 mmol); methanol (50 mmol); catalyst (50 mg); temperature (298 K); runtime (2 h).

20 mA) and a proportional counter detector. Nitrogen adsorption measurements at 77 K were performed by using a NOVA 1000 series Quantachrome Instruments volumetric adsorption analyzer. The samples were out-gassed at 573 K for 4 h before the adsorption measurement. The specific surface area was determined by the BET method using the data points of P/P_0 in the range of about 0.05–0.3. The pore size distribution was estimated by using the Barret–Joyner–Halenda (BJH) model. Scanning electron microscopy (SEM) images were obtained by means of a Hitachi S-4300 F instrument. Small amount of sample was mounted on carbon tape and then coated with evaporated gold prior to imaging. Transmission electron microscopy (TEM) images were obtained by means of a Hitachi H-800 instrument with a working voltage of 200 kV. The calcined sample was dispersed in ethanol, mounted on a Cu grid, dried, and used for TEM measurement. Solid-state NMR experiments were performed by using a Bruker DSX300 spectrometer with a frequency of 59.63 MHz, a recycling delay of 600 s, and a radiation frequency intensity of 62.5 kHz. Temperature-programmed desorption (TPD) experiments were conducted by using a TPD-1-AT instrument (BEL Japan). In a typical experiment, 250 mg of sample was placed in a U-shaped, flow-through, quartz sample tube. Before the TPD experiments, the catalyst was pretreated in He ($50\ cm^3 min^{-1}$) at 823 K for 1 h. After cooling down to 373 K, ammonia (partial pressure 100 Torr) was adsorbed on the samples for 1 h. The sample was subsequently flushed by He stream ($50\ cm^3 min^{-1}$) at 373 K for 1 h to remove physisorbed ammonia. The TPD experiments were carried out in the range of 373–873 K at a heating rate of $10\ K min^{-1}$. The ammonia concentration in the effluent was monitored by using a gold-plated, filament thermal conductivity detector.

All the catalytic reactions were performed in a Teflon-lined steel autoclave. In a typical alkylation reaction, toluene (50 mmol), benzyl chloride (5 mmol) and catalyst (100 mg) were mixed and the reaction was conducted at 413 K for 2 h. The reaction mixture was analyzed by gas chromatography. In a typical Claisen–Schmidt condensation reaction for the synthesis of flavonone/chalcone, 2′-hydroxy acetophenone (7 mmol), benzaldehyde (7 mmol) and catalyst (pre-activated at 423 K, 100 mg under vacuum) were mixed and the reaction was conducted at 423 K for 8 h. The products were dissolved by adding a small amount of acetone to the reaction mixture and were analyzed by gas chromatography. In the synthesis of 7-hydroxy-4-methyl-coumarin, resorcinol (5 mmol), ethylacetoacetate (7.5 mmol), and catalyst (pre-activated at 423 K, 100 mg) were mixed and the reaction was conducted at 423 K for 4 h. The products were dissolved by adding a small amount of acetone to the reaction mixture and were analyzed by gas chromatography. In the protection reaction, cyclohexanone (0.98 g, 10 mmol) and methanol (3.2 g, 100 mmol) were charged with catalyst (0.1 g) in a 25 mL round bottom flask. The reaction was carried out at 298 K for 2 h under magnetic stirring. Products were identified by using a GC-MS (Shimadzu GCMS-QP5050) and authentic samples obtained from Aldrich. Quantitative determinations were based on the measured response factors of the reactants and products.

Acknowledgements

The authors wish to express their thanks to Japan Society for the Promotion of Science for JSPS postdoctoral fellowship for R.S. (P07130) and for Grant-in-Aid for JSPS fellows (19·07130). The authors are thankful to Mr. Y. Nodasaka for TEM measurements and Mr. Yamada for NMR analysis.

Keywords: hydrothermal synthesis · mesoporous zeolite · MFI zeolite · morphology · nanocrystalline zeolite

[1] a) J. Cejka, H. Van Bekkum, *Zeolites and Ordered Mesoporous Materials: Progress and Prospects, Studies in Surface Science and Catalysis 157C*, Elsevier, Amsterdam, **2005**; b) E. Van Steen, M. Claeys, L. H. Callanan, *Recent Advances in the Science and Technology of Zeolites and Related Materials, Studies in Surface Science and Catalysis 154B*, Elsevier, Amsterdam, **2005**; c) A. Corma, H. Gracia, *Chem. Rev.* **2003**, *103*, 4307–4366; d) J. A. van Bokhoven, A. M. J. van der Eerden, R. Prins, *J. Am. Chem. Soc.* **2004**, *126*, 4506–4507.

[2] A. Corma, *Chem. Rev.* **1997**, *97*, 2373–2420.

[3] a) S. van Donk, A. H. Janssen, J. H. Bitter, K. P. de Jong, *Catal. Rev. Sci. Eng.* **2003**, *45*, 297; b) S. Bernasconi, J. A. van Bokhoven, F. Krumeich, G. D. Pirngruber, R. Prins, *Microporous Mesoporous Mater.* **2003**, *66*, 21–26.

[4] A. H. Janssen, A. J. Koster, K. P. de Jong, *Angew. Chem.* **2001**, *113*, 1136–1138; *Angew. Chem. Int. Ed.* **2001**, *40*, 1102–1104.

[5] a) C. J. H. Jacobsen, C. Madsen, J. Houzvicka, I. Schmidt, A. Carlsson, *J. Am. Chem. Soc.* **2000**, *122*, 7116–7117; b) Z. Yang, Y. Xia, R. Mokaya, *Adv. Mater.* **2004**, *16*, 727–733; c) Y. Tao, H. Kanoh, K. Kaneko, *J. Am. Chem. Soc.* **2003**, *125*, 6044–6045; d) M. Hartman, *Angew. Chem.* **2004**, *116*, 6004–6006; *Angew. Chem. Int. Ed.* **2004**, *43*, 5880–5882.

[6] M. Choi, H. Cho, R. Srivastava, C. Venkatesan, D. Choi, R. Ryoo, *Nat. Mater.* **2006**, *5*, 718–723.

[7] R. Srivastava, M. Choi, R. Ryoo, *Chem. Commun.* **2006**, 4489–4491.

[8] a) H. Wang, T. J. Pinnavaia, *Angew. Chem.* **2006**, *118*, 7765–7768; *Angew. Chem. Int. Ed.* **2006**, *45*, 7603–7606; b) C. H. Christensen, K. Johannsen, I. Schmidt, C. H. Christensen, *J. Am. Chem. Soc.* **2003**, *125*, 13370–13371; c) M. Kustova, K. Egeblad, K. Zhu, C. H. Christensen, *Chem. Mater.* **2007**, *19*, 2915–2917; d) D. P. Serrano, J. Aguado, J. M. Escola, J. M. Rodríguez, A. Peral, *Chem. Mater.* **2006**, *18*, 2462–2464; e) F.-S. Xiao, L. Wang, C. Yin, K. Lin, Y. Di, J. Li, R. Xu, D. S. Su, R. Schlögl, T. Yokoi, T. Tatsumi, *Angew. Chem.* **2006**, *118*, 3162–3165; *Angew. Chem. Int. Ed.* **2006**, *45*, 3090–7093.

[9] N. Kröger, R. Deutzmann, M. Sumper, *Science* **1999**, *286*, 1129–1132.

[10] S. R. Qiu, A. Wierzbicki, E. A. Salter, S. Zepeda, C. A. Orme, J. R. Hoyer, G. H. Nancollas, A. M. Cody, J. J. De Yoreo, *J. Am. Chem. Soc.* **2005**, *127*, 9036–9044.

[11] a) X. Wang, Y.-H. Tseng, J. C. C. Chan, S. Cheng, *J. Catal.* **2005**, *233*, 266–275; b) M. T. Drexler, M. D. Amiridis, *J. Catal.* **2003**, *214*, 136–145.

[12] a) R. Sabou, W. F. Hoelderich, D. Ramprasad, R. Weinand, *J. Catal.* **2005**, *232*, 34–37; b) E. A. Gunnewegh, A. J. Hoefnagel, H. van Bekkum, *J. Mol. Catal. A* **1995**, *100*, 87–92.

[13] a) T. W. Bastock, J. H. Clark, *Speciality Chemicals*, Elsevier, London, **1991**; b) B. M. Khadilkar, S. D. Borkar, *J. Chem. Technol. Biotechnol.* **1998**, *71*, 209–215; c) A. D. Harford, H. W. Vernon, US Patent 2897112, **1956**.

Received: June 9, 2008
Published online: September 12, 2008

